RSC Advances

PAPER

View Article Online
View Journal | View Issue

Cite this: *RSC Adv.*, 2020, **10**, 8480

Construction of octenyl succinic anhydride modified porous starch for improving bioaccessibility of β-carotene in emulsions†

Haiyan Li,‡[a] Yunxiang Ma,‡[a] Liyue Yu,[a] Huadong Xue,[b] Yue Wang,[a] Jinfeng Chen[a] and Shenggui Zhang *[a]

Received 2nd December 2019
Accepted 24th January 2020

DOI: 10.1039/c9ra10079b

rsc.li/rsc-advances

Modified porous starch (PS), by introducing octenyl succinic anhydride (OSA) moieties, was synthesized successfully, which was applied as an emulsion of β-carotene for the first time. The pores and channels within porous starch provided more possibilities for OSA to modify starch. The ester linkage of OSA modified PS with different degrees of substitution (DS) were confirmed by both ^{13}C solid-state NMR and Fourier transform-infrared spectroscopy (FT-IR). The hydrophobic octenyl succinic and hydrophilic hydroxyl groups of OSA modified PS showed the good emulsifying capability, which could be utilized to prepare β-carotene emulsions. And the bioaccessibility of β-carotene was also enhanced with increasing DS of OSA modified starch. This study not only paves a new way using porous starches for modification of starch, but also offers an attractive alternative for obtaining emulsion-based delivery systems for bioactive components.

1. Introduction

Over the last decades, great efforts have been devoted to the association between diet and chronic diseases. Based on the convincing evidence from scientific research, the consumption of fruits and vegetables, which are good sources of carotenoids and other bioactive compounds, plays an important role in the prevention of human diseases.[1] carotenoids, including β-carotene, lutein and neoxanthin, represent a large family of tetraterpenoid organic pigments, which are widely found in various colorful fruits and vegetables.[2,3] As one type of carotenoid, β-carotene showed highly desirable bioactivities such as health-promoting properties, and antioxidant activity, which can maintain human health and prevent chronic diseases including cardiovascular diseases, cancer and other chronic diseases.[4,5] Due to the low stability, solubility and bioaccessibility, the supplemented foods of β-carotene were greatly limited.[3–6] It was worth noting that utilization of an emulsion-based delivery system is considered as an effective method for overcoming the limitations of β-carotene. The conventional emulsifying agent, including Tween 20, and polyglycerol esters,[7–9] showed the excellent ability of emulsification for fabrication of colloidal system. For example, Tween 20 has been applied as an emulsifier to prepare β-carotene nano-dispersions for the first time by Tan *et al.* However, the chemical emulsifiers may pose a potential threat to human health in the field of foods and beverages, especially for the consumption at high-level.[10] With an increasing concern on the safety of the delivery system, there is an increasingly urgent need to search for a safe emulsifier as a candidate. Emulsions from biopolymers of plants and microbial, possessing higher safety in food-grade, are considered as potential alternatives for fabrication of emulsions.[3] The application of biopolymer-based emulsifiers was labeled as plant sources surfactants than the synthetic and semi-synthetic one.[11] Previous research suggested that biopolymer emulsifiers, including proteins[12] and polysaccharides,[13] have been applied for the fabrication of the delivery system of carotenoid successfully. Among these food-grade biopolymer emulsifiers, starches chemically modified by different alkenyl succinic anhydrides, possessing the favorable hydrophobicity, are suitable to stabilize emulsions.[14] For example, octenyl succinic anhydride modified starch, which is synthesized by esterification between the hydroxyl group of the starch and the carboxyl group of OSA, has also been utilized for preparing β-carotene emulsions due to its strong surface activity and good emulsifying properties.[3,14,15] Various studies indicated that hydrophobic octenyl and carboxyl groups, derived from OSA modified starch, can improve the emulsifying capability of starch.[16,17] Meanwhile, the degree of substitution has also a great influence on the emulsification effect of OSA modified starch. It has been proved that the emulsions with the larger DS exhibited the less

[a]*College of Food Science and Engineering, Gansu Agricultural University, No. 1 Yingmencun, Anning District, Lanzhou 730070, Gansu, China. E-mail: zhangshenggui@gsau.edu.cn*

[b]*State Key Laboratory of Applied Organic Chemistry, College of Chemistry and Chemical Engineering, Lanzhou University, Lanzhou 730000, Gansu, China*

† Electronic supplementary information (ESI) available. See DOI: 10.1039/c9ra10079b

‡ Haiyan Li and Yunxiang Ma contributed equally to this work.

flocculation and coalescence.[18,19] It is well known that the DS of OSA modified starch is greatly affected by the process of esterification.[20] However, the esterification reaction of OSA modified starch was restricted by the naturally low surface areas of starch, which resulted in the low DS.[21] Therefore, exploring the efficient approach with more reactive sites for esterification is a great challenge in this field. It was worth noting that, porous starch is a type of well-known modified starch, which have the high surface areas[22,23] to overcome the above limitation of native starches.

Porous starch, obtained by the physical, chemical, and enzyme treatment, is a modified starch with abundant pores, which extended from the surface to the center of starch granules.[24] Derived from these micro-sized pores and channels, porous starch possessed the larger specific surface area, which showed the more chemically reactive sites than that of starch.[22,23,25] Many studies also proved that the modification of porous starch gives a higher DS than the native one.[23] The pores and channels within porous starch provided more possibilities for chemical agents to penetrate easily into the interior of starch for further modifications. Therefore, the higher DS of esterified starch could be obtained using porous starch instead of the native one. Porous starch may be very suitable as a host material for further OSA modification. To the best of our knowledge, few researches have been reported about the fabrication and application of OSA modification using porous starch.

In this study, porous starch modified by introducing OSA moieties was synthesized successfully, which was applied as an emulsion of β-carotene for the first time. As shown in Fig. 1, the schematic illustration was exhibited to illustrate entire process. Porous starch synthesized by enzymatic hydrolysis, was modified by esterification with OSA groups to form OSA modified porous starch (OSA@PS). In comparison with native starch (NS), PS has the larger surface areas, which could offer more reaction sites. Thus, at the same experimental condition, the greater DS of OSA modified starch should be obtained using PS instead of NS. The successful formation of the ester linkage was confirmed by both ^{13}C solid-state NMR spectroscopy and FT-IR. The crystalline and porous structures were characterized by X-ray diffraction analysis (XRD) and scanning electron microscopy (SEM) respectively. Furthermore, OSA modified porous starch was applied as the emulsifier to fabricate β-carotene emulsions. By mimicking digestion process in oral, gastric and intestinal fluid, the digestion test *in vitro* was carried out to determine the bioaccessibility of β-carotene after emulsions.

2. Materials and methods

2.1 Materials

Corn starch, α-amylase (AM, 50 U mg^{-1}), amyloglucosidase (AMG, 100 U mL^{-1}), octenyl succinic anhydride, were purchased from Shanghai Yuanye Biotechnology Co., Ltd. All the reagents used were of analytical grade unless otherwise stated.

2.2 Methods

2.2.1 Preparation of porous starch. The porous starch was prepared according to the reported procedures[24] with a slight modification: native corn starch (10.0 g) was suspended in 60 mL phosphate buffer at pH 6.6 and in 20 mL acetate mixed buffer at pH 4.5, stirred in a water bath at 40 °C for 20 min. The mixed enzyme, whose ratio of α-amylase (50 U mg^{-1}) and amyloglucosidase (100 U mL^{-1}) was 6 : 1, were added into the suspension. The samples were kept in a shaking water bath at 50 °C for 24 h. Then, the pH was adjusted to 10.0 by adding 1 M NaOH solution. The suspension was centrifuged and washed using the distilled water. Finally, the collected precipitate was dried at 50 °C to yield the porous starch. The product was ground through a 90 mesh sieve in a desiccator for further use.

2.2.2 Preparation of OSA modified NS and PS. OSA modified NS or PS samples was prepared according to the previous method of Song *et al.*[26] Corn starch or porous starch (5 g) was suspended in water (30%, w/w). The pH of suspension was adjusted to 8.5 by the addition of 3% NaOH solution. 3% and 5% OSA solution, diluted with ethanol, were added dropwise to

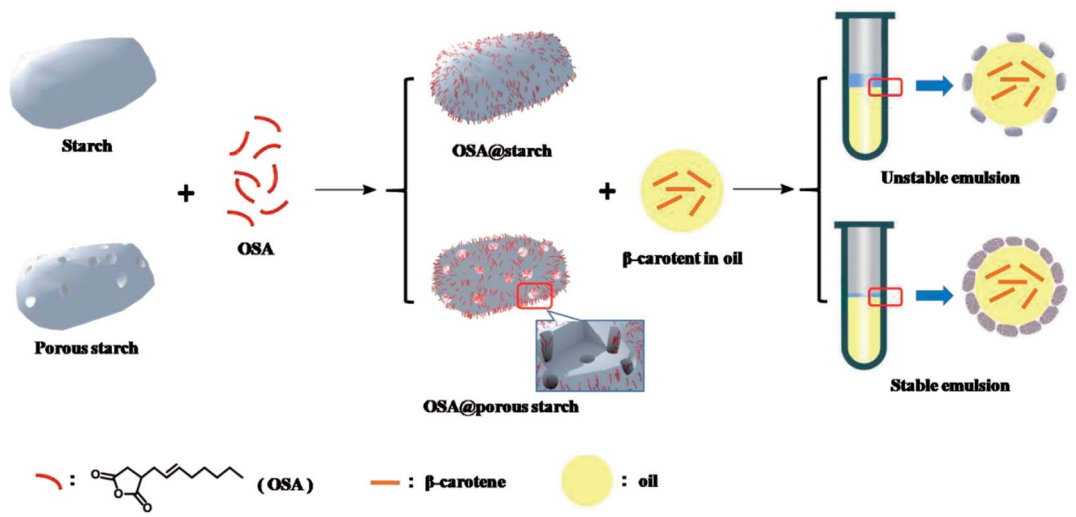

Fig. 1 Schematic representation of synthesis and application of OSA modified porous starch and native starch.

the starch slurry within 2 h respectively. The reaction was maintained at 35 °C for 1 h, and then the pH was adjusted to 6.5. The mixture was centrifuged and washed with water and ethanol respectively. The precipitation was dried at 40 °C to yield the modified starches. The products were subsequently referred to as 3% OSA modified native starch (3% OSA@NS) and 5% OSA@NS, 3% OSA modified porous starch (3% OSA@PS) and 5% OSA@PS, respectively.

2.2.3 Determination of degree of substitution. The DS was measured according to the titration method described by Song *et al.*[26] DS was calculated using the following formula:

$$\mathrm{DS} = \frac{162(A \times M)/W}{1000 - 210(A \times M)/W} \quad (1)$$

where 162 is the molar mass (g mol^{-1}) of the glucose residue, 210 is the molar mass of OSA, A represents the titration volume (mL) of the NaOH solution, M represents the molar concentration (mol L^{-1}) of the NaOH solution, and W represents the dry weight (g) of sample.

Free OSA content of OSA modified starches was measured by ^{1}H NMR experiments referred to the method of Tizzotti *et al.*[27]

2.2.4 Structural characterization analysis of modified starch

2.2.4.1 ^{13}C solid-state NMR spectroscopy. Solid-state NMR measurements were carried out on a Bruker WB Avance II 400 MHz spectrometer. The transmitter frequency of ^{13}C NMR is 100.60 MHz. The solid-state ^{13}C cross-polarization magic angle spinning (CP/MAS) NMR spectra were recorded with a 4 mm double-resonance MAS probe and with a spinning rate of 10.0 kHz; a pulse delay of 3 s was applied during data acquisition with a contact time of 2.5 ms (ramp 100). The ^{13}C chemical shifts were referenced to the signal of tetramethylsilane as 0 ppm.

2.2.4.2 Fourier transform-infrared spectroscopy. The FT-IR spectra of NS, PS, OSA@NS and OSA@PS were determined by FT-IR spectroscopy (Nicolet NEXUS 670, American). Scanning was performed from 4000–450 cm^{-1} at a resolution of 4 cm^{-1}.

2.2.4.3 X-ray diffraction analysis. The crystal structures of NS, PS, OSA@NS and OSA@PS were characterized by X-ray diffract meter (Shimadzu, XRD-6000, Japan). The test conditions were as follows: voltage: 40 kV; current: 40 mA; scanning speed: 2° min^{-1}; scanning step size: 0.06°; scanning method: continuous. The relative crystallinity (%) was quantified as the ratio of the crystalline area to the total area under the diffractogram.

2.2.4.4 Scanning electron microscopy. The morphology of NS, PS, OSA@NS and OSA@PS were observed using an SEM instrument (JSM-6701F, Electron Optics Inc., Japan). The shape and surface characteristics of the samples were observed at an accelerating voltage of 5 kV.

2.2.5 Preparation of emulsions. For the preparation of emulsions, the reported method of Lin *et al.*[19] was used and appropriately modified as follows: the OSA modified starch (5%, w/w) was suspended in Milli-Q water and stirred in a boiling water bath for 20 min. Then 1.17 mL corn oil containing 0.1% (w/w) β-carotene was added starch gel to obtain a final mixture with 5% (w/w) OSA modified starch and 10% (w/w) oil. The crude emulsion was passed through an ultrahigh pressure homogenizer (Scientz-207A, China) at a mean value of 130 MPa for 2 min with three cycles to prepare an emulsion. All of devices and beakers were wrapped with aluminum foil to avoid light exposure during preparation.

2.2.6 *In vitro* digestion of emulsion. Simulated saliva fluid (SSF) was prepared refer to the method of Hur *et al.*[28] with appropriate modifications, containing α-amylase and various salts except mucin. Simulated gastric fluid (SGF) and simulated small intestinal fluid (SIF) were prepared according to the literatures.[11,29]

2.2.7 Particle size measurements. The particle size distribution of the emulsion was measured using a laser particle size distribution analyzer (Bettersize 2600, China). The result is expressed as the surface area average diameter d_{32}, which is defined as $\Sigma n_i d_i^3/\Sigma n_i d_i^2$.

2.2.8 Confocal laser scanning microscopy (CLSM). The microstructure of the emulsion was observed using CLSM (Confocal Laser Scanning Microscope, LSM800, Germany). Samples (1 mL) were dyed with 0.5% Nile Red solution. Then, samples were observed by the 63× oil immersion objective lens, with the excitation light of 561 nm (argon), at the reflection wavelength of 525–618 nm. Images were acquired and processed using digital image processing software Leica LAS AF.

2.2.9 Determination of bioaccessibility of β-carotene. After the simulated digestion process, samples were collected and centrifuged at 8000 rpm to obtain three phases. The upper, middle and bottom layer were attributed to thin oil layer, micelle phase and insoluble precipitate respectively. After taking 5 mL of micelle phase through a 0.45 μm microporous membrane, β-carotene was extracted and measured according to the reported method.[30] The filtrate was mixed with dimethyl sulfoxide in equal volumes and destructed the structure of emulsion by vortex oscillator process. Next, dichloromethane/*n*-hexane (1 : 4, v/v) was added, and centrifuged at 4000 rpm. The bottom yellow layer was analyzed by spectrophotometer at 450 nm. The concentration of β-carotene in the original emulsion and micellar phase were determined from a calibration curve.

$$\text{Bioaccessibility (\%)} = \frac{\text{amount of solubilized β-carotene in mixed micelles}}{\text{amount of β-carotene in the formulations}} \times 100 \quad (2)$$

2.2.10 Statistical analysis. The whole experiments were assayed in duplicate with triplicate measurements being made on each sample, and the results were expressed as the mean and

standard deviation. The one-way analysis of variance (ANOVA) test was analyzed using the SPSS 22.0 package. Duncan's multiple range test was used to determine the significant differences of the mean values ($p < 0.05$).

3. Results and discussion

3.1 DS of OSA modified NS and PS

The OSA@NS and OSA@PS possessing different DS were synthesized according to the methods above. With varying the ratio of OSA to NS and PS from 3% to 5%, the DS of OSA@NS was changed from 0.0195 to 0.0289. The DS was enhanced as the increasing concentration of OSA, which showed a similar trend in OSA-treated ginkgo starch.[31] It could be interpreted that greater availability of OSA molecules was in the proximity of starch molecule during esterification.[32] In comparison with NS, OSA@PS has a larger DS (Table 1), which was proved by the result from ^{1}H NMR of free OSA (ESI Table S1 and Fig. S1†). It was derived from additional pores and channels within the porous starch structure, which provides a larger specific surface area and more reactive sites with OSA.

Table 1 The DS and relative crystallinity (X_c) of varied OSA modified starches[a]

Samples	DS	X_c (%)
NS	0	31.84 ± 0.1380^b
PS	0	30.18 ± 0.1751^b
3% OSA@NS	0.0195 ± 0.0195^d	33.28 ± 0.0980^a
5% OSA@NS	0.0228 ± 0.0162^c	31.95 ± 0.1310^a
3% OSA@PS	0.0260 ± 0.0249^b	28.83 ± 0.1551^c
5% OSA@PS	0.0289 ± 0.0205^a	28.22 ± 0.0616^c

[a] Values are given as mean ± standard deviation. Different superscript letters in the columns indicate significant difference ($p < 0.05$).

3.2 Structural characterization of modified NS and PS

3.2.1 ^{13}C solid-state NMR spectra. To confirm the formation of ester linkage between porous starch and OSA during the esterification reaction, solid-state ^{13}C CP/MAS NMR analysis was performed on porous starch and OSA modified one (DS = 0.0289) as shown in Fig. 2a and b. In the high field, the peaks centered at 63.5 ppm, 70.5–81.7 ppm and 101.2 ppm were attributed to the signals of C-6, C-2, 3, 4, 5 and C-1 of starch respectively.[33] The spectrum of OSA@PS was almost identical to that of PS in high field, indicating the structural preservation after esterification reaction. It was worth noting that the partially enlarged solid-state ^{13}C spectrum of OSA@PS from 120 to 250 ppm was also embedded in Fig. 2c. The peak centered at 174 ppm was observed obviously, which was derived from ^{13}C chemical shift of ester linkage.[34] This result indicated that the atomic-level linkages between OSA and PS were constructed successfully through esterification. ^{13}C CP/MAS NMR spectrum of NS was almost identical to that of PS, indicating that enzymatic hydrolysis has no influence on the skeleton of starch at atomic level. Due to the low DS of OSA modified starch and limited resolution of solid-state NMR, the effect of enzymatic hydrolysis on the efficiency of esterification could not be evaluated between NS and PS

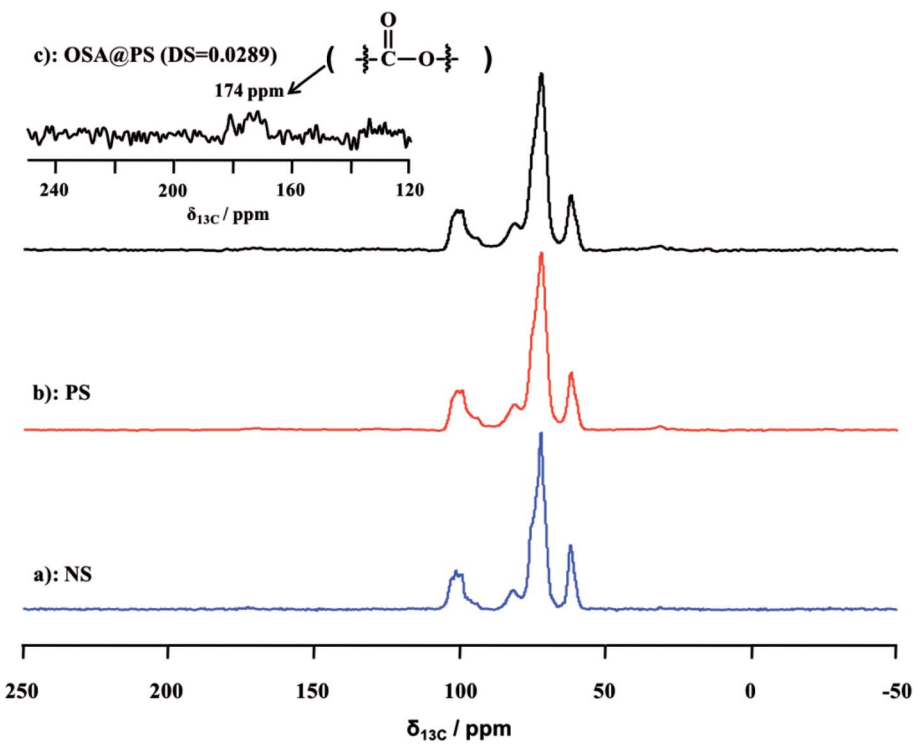

Fig. 2 Solid-state ^{13}C CP/MAS NMR spectra of NS (a), PS (b) and OSA modified PS (c). The peak at 174 ppm was attributed to the ester linkage, indicating that OSA modified PS was obtained successfully.

accurately. Fortunately, this issue could be solved by FT-IR spectroscopy successfully.

3.2.2 Fourier transform-infrared spectroscopy. Meanwhile, the ester formation was also confirmed in OSA modified PS by FT-IR spectroscopy. The FT-IR spectra of NS, PS, OSA@NS and OSA@PS were shown in Fig. 3. FT-IR spectrum of NS was almost identical to that of PS, indicating that enzymatic hydrolysis has no influence on the skeleton of starch. Compared with the spectra of non-esterified NS and PS, two new absorption bands at 1725 and 1570 cm^{-1}, which were corresponding to the C=O and RCOO– group of the ester, were observed obviously in that of OSA modified NS and PS.[35,36] Meanwhile, the signal became increasingly obvious with the raising DS gradually. Compared FT-IR spectra of OSA@NS and OSA@PS, it was worth noting that adsorption bands of C=O (1725 cm^{-1}) and RCOO– (1570 cm^{-1}) of OSA@PS could be observed obviously than that of OSA@NS in FT-IR spectra. This result suggested that enzymatic hydrolysis improved the efficiency of esterification, due to the larger surface areas of PS. This result, which offered the further evidence for the formation of ester linkage, indicated that OSA was successfully introduced into NS and PS by means of esterification reaction.

3.2.3 X-ray diffraction analysis. To verify the crystalline structure of OSA modified starch before and after esterification reaction, the XRD analysis was carried out on NS, PS, OSA@NS and OSA@PS, as shown in Fig. 4. The XRD patterns of all samples, with diffraction peaks at 15°, 17°, 18° and 23°, were attributed to the typical A-type crystalline structure. In comparison with PS, the XRD pattern of OSA@PS was almost identical to that of PS (Fig. 4d–f), indicating that the crystalline structure was still maintained after esterification. A similar phenomenon has also been observed in the case of OSA@NS (as shown in Fig. 4a–c), suggesting that crystalline structure of starch cannot be destroyed by modification of OSA.[37] No significant differences were noted between NS and PS of X_c (Table 1), meanwhile, the crystallinities of the porous starches were almost consistent with their esters.[38] This indicates that the crystalline patterns of the starches were not changed by OSA esterification.[32]

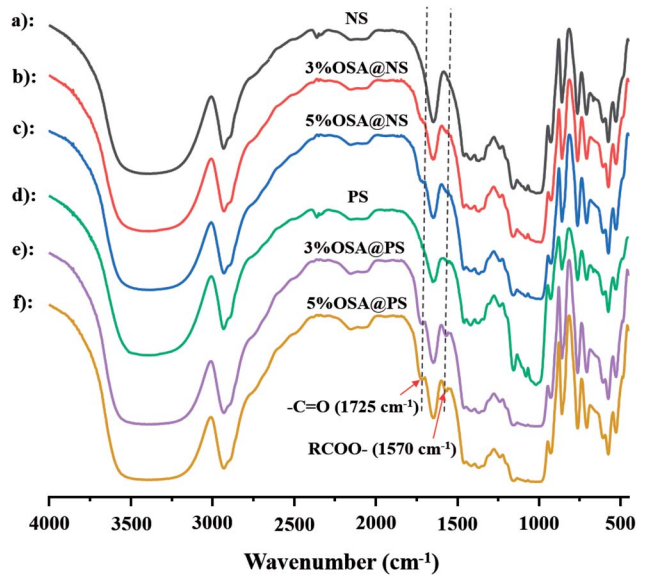

Fig. 3 FT-IR spectra of starch and OSA modified starches ((a) NS; (b) 3% OSA@NS; (c) 5% OSA@NS; (d) PS; (e) 3% OSA@PS; (f) 5% OSA@PS). The bands of OSA modified starch at 1725 cm^{-1} and 1570 cm^{-1} correspond to the stretching vibration of C=O and the asymmetric stretching vibration of RCOO–, indicating the successful formation of the ester linkage.

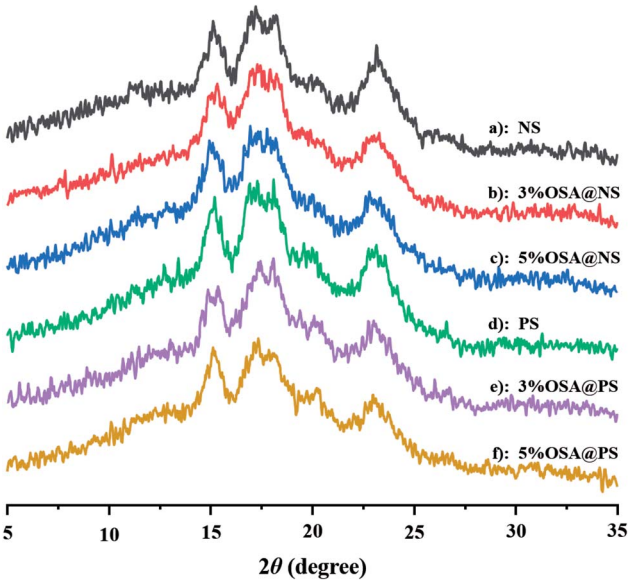

Fig. 4 XRD patterns of OSA modified starches ((a) NS; (b) 3% OSA@NS; (c) 5% OSA@NS; (d) PS; (e) 3% OSA@PS; (f): 5% OSA@PS). The result indicated that the crystalline structure was still maintained after esterification.

3.2.4 Scanning electron microscopy. Furthermore, the pore morphology of PS and OSA@PS, with magnification of 2000 times, was eventually verified by SEM analysis before and after esterification. The SEM image of NS (Fig. 5a) showed an irregular and polygonal shape with relatively smooth surface. After esterification, the surface of starch granules becomes rougher (Fig. 5b) than NS.[39] As shown in Fig. 5c, many pores and cavities were observed obviously due to the enzymatic hydrolysis. These porous structures offered more chemical reactive sites than NS, due to the larger specific surface area. It was also proved that the porous starch was more suitable for chemical modification than the native one. The SEM image of OSA@PS was displayed in Fig. 5d. Many pores and channels, with slight corrosion, were still maintained, indicating that the porous structure was not destroyed after esterification.[22] The high-resolution SEM analysis with magnification of 4000 times was performed on the PS and OSA@PS, as shown in Fig. 5e and f respectively. These images showed the porous structures more clearly before and after esterification, suggesting that pores and channels were still maintained after post-treatment.

N_2 adsorption analysis was also utilized to explore porous structure of PS before and after esterification. The application of the Brunauer–Emmett–Teller (BET) model resulted in the surface areas of 1.08 and 1.43 $m^2\ g^{-1}$ for PS (ESI Fig. S2†) and

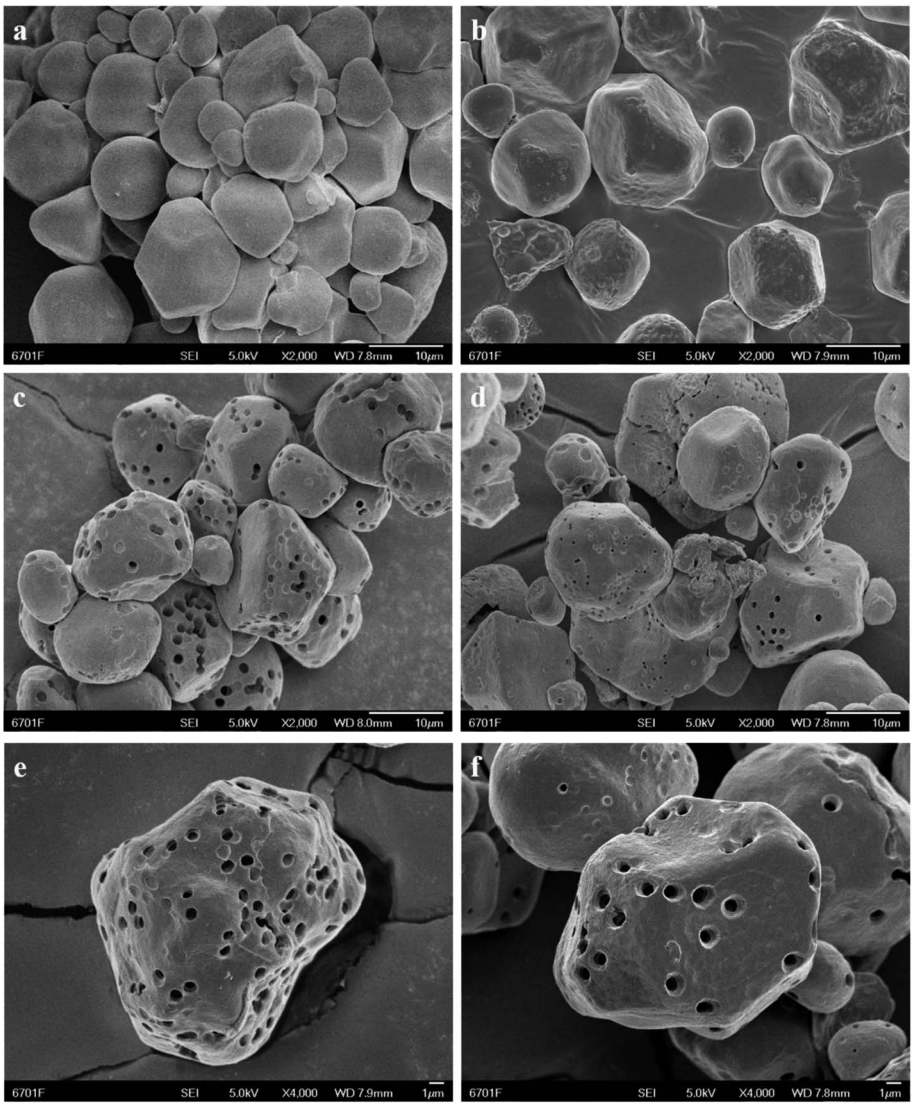

Fig. 5 SEM images of NS (a) and OSA@NS (b), images of PS (c) and OSA@PS (d), images of PS with magnification of 4000 times (e) and OSA@PS with magnification of 4000 times (f). The SEM image of OSA@PS after esterification showed the undamaged pores and channels obviously, indicating that porous structure was still maintained after post-treatment.

5% OSA@PS (ESI Fig. S3†), respectively. In comparison with the case of PS, no difference was observed obviously indicated that pores within PS were still maintained after esterification.

3.3 Effect of modified starch on digestion characteristics of emulsion

3.3.1 Initial emulsion. Particle size distribution analysis was a significant tool for detecting the sizes of emulsions, which was expressed by the key parameter of d_{32}. As shown in Fig. 6 and 7, the mean sizes of emulsion, stabilized by OSA modified starch, during digestion were studied by particle size distribution analysis. The particle sizes of initial emulsions showed a narrow monomodal distribution centered at about 0.75 μm (Fig. 7). Displayed in black histogram of Fig. 6, compared with the particle sizes of two OSA@NS samples, the emulsion prepared by 3% OSA@PS, with the DS of 0.026 showed the slightly smaller particle size. However, when the DS of OSA@PS was raised up to 0.0289, the particle size of emulsion became larger than that of 3% OSA@PS. This result may be derived from the greater loading amount of OSA groups would result in the larger steric hindrance of the interfacial layer.[40] The confocal images (Fig. 8) also offered the evidence that the initial emulsions of OSA@NS and OSA@PS possessed the small particle sizes. Furthermore, oil droplets of initial emulsions showed the uniform distribution, with only a few amounts of large oil droplets, which is consistent with the particle size measurement above.

3.3.2 Mouth phase. No significant change of average particle size distributions was observed during all emulsions moved through the SSF, as shown in Fig. 6 and 7. Meanwhile, confocal microscopy images also showed that the sizes of oil droplets in the emulsion were still maintained after incubation in the mouth. The results were attributed to effect of protection, which oil droplets embedded with OSA modified starches could

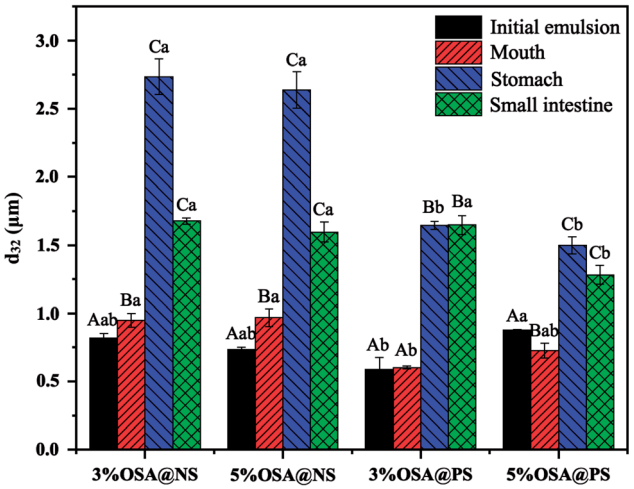

Fig. 6 Particle size (d_{32}) of emulsions containing β-carotene during *in vitro* digestion. Different capital letters indicate significant differences ($p < 0.05$) in the droplet diameter of an emulsion between digestion phases. Different lowercase letters indicate significant differences ($p < 0.05$) in the droplet diameter between emulsions within the same digestion phase.

avoid the attack of mineral ions and α-amylase in SSF.[29] OSA modified starches have the spatial repulsion generated by its branched structure, which could resist the attack of ionic strength and α-amylase.[3] Moreover, the short residence time and low consumption of starch in the oral cavity would not result in a significant change in the structure of emulsions.

3.3.3 Stomach phase. The particle size distribution of the emulsions was measured after treatment of SGF, as shown in the blue histogram of Fig. 6. Compared with the SSF (seen the red histogram of Fig. 6), the particle sizes of emulsions were increased significantly after 1 h in SGF. This observation, which was consistent with the result of research,[19] may result from the flocculation and coalescence occurred in the SGF.[41] The variation of particle size distribution showed narrower extent in OSA@PS than that of OSA@NS. Meanwhile, as shown in the blue triangle-label of Fig. 7, in comparison to the bimodal distributions of OSA@NS (Fig. 7a and b) with the scope of 0.1–10 μm, the narrow monomodal distributions of OSA@PS was observed obviously (Fig. 7c and d) with the scope of 0.1–1 μm. This result indicated that the OSA@PS exhibited the excellent stability of the emulsions than that of NS.[42]

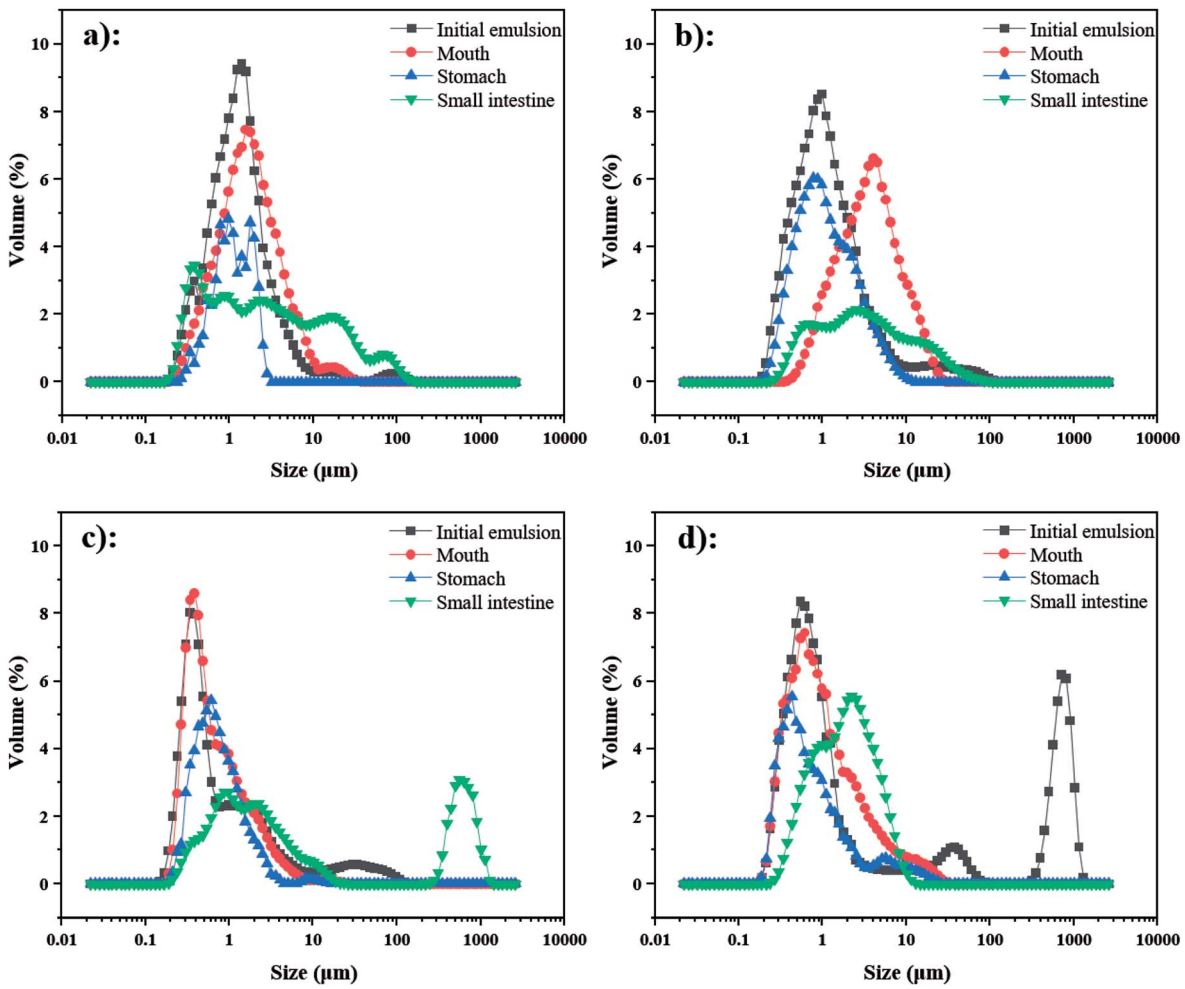

Fig. 7 Particle size distribution of emulsions containing β-carotene during *in vitro* digestion ((a) 3% OSA@NS; (b) 5% OSA@NS; (c) 3% OSA@PS; (d) 5% OSA@PS).

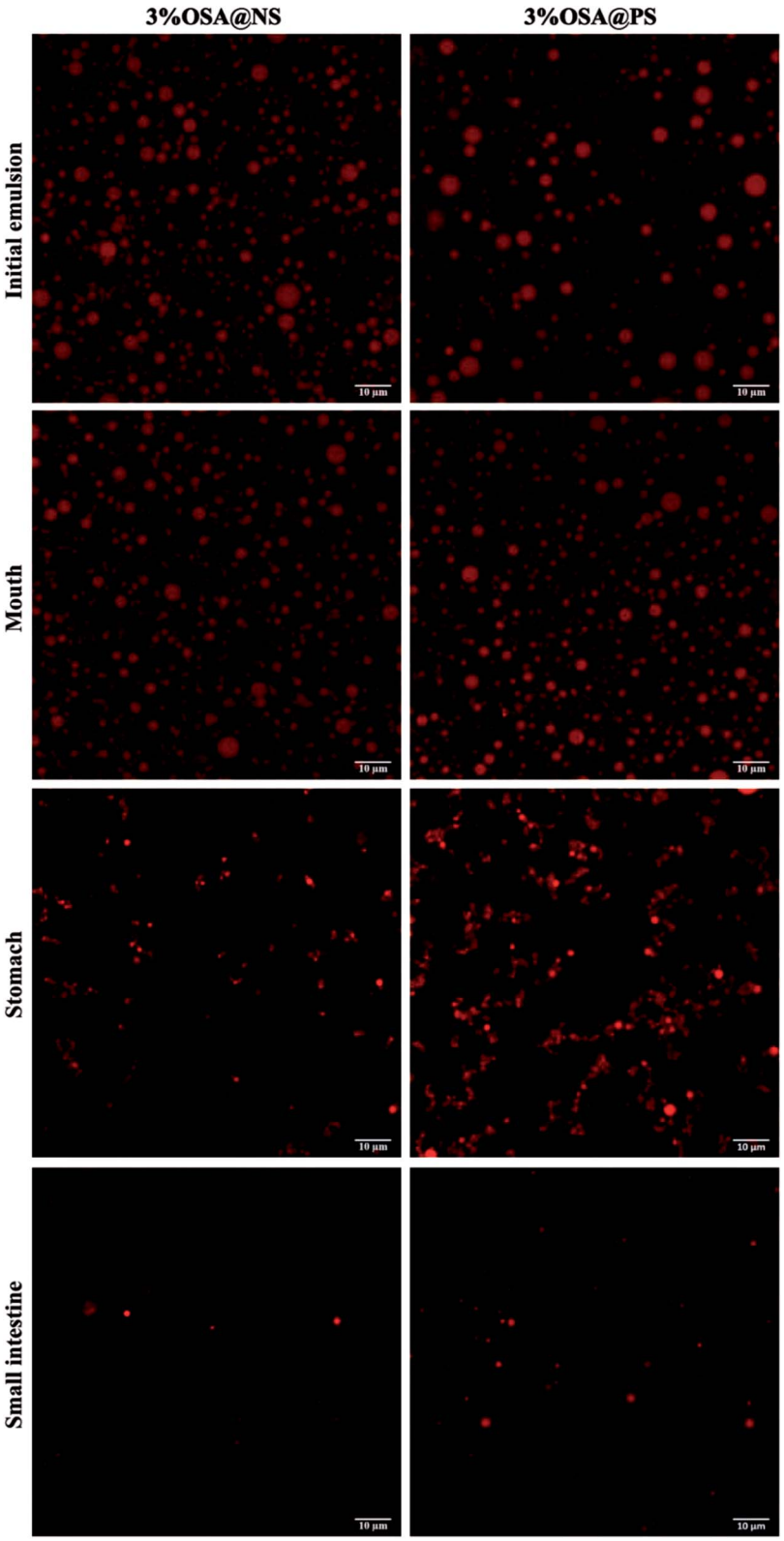

Fig. 8 Changes in the microstructure (determined by CLSM) of emulsions containing β-carotene during *in vitro* digestion.

As shown in ESI Fig. S4,† by means of CLSM analysis, the variation of microstructure was observed obviously in all emulsions after SGF. In the emulsions stabilized by OSA@NS, many flocs appeared along with the disappearance of small oil droplets, which indicated that severe flocculation and coalescence occurred in these emulsions.[18] However, only a few flocs

and large particles were observed in OSA@PS, which showed the greater stability than that of OSA@NS. This phenomenon may be explained that OSA@PS with higher DS provided a large amount of OSA groups, which not only had the larger steric hindrance, but also formed the more rigid and dense interface layer.[18,43]

3.3.4 Small intestine phase. The particle size distribution of the emulsions was measured after treatment of SIF for two hours. As shown in the green histogram of Fig. 6, the particle sizes of emulsions decreased slightly, in the confocal microscopy images, the sizes and amount of oil droplets in all the samples were obviously reduced, compared to that of SGF. Previous studies have already offered the evidence that the sizes and amount of oil droplets would decrease after digestion *in vitro*.[29]

3.4 Determination of bioaccessibility of β-carotene

For better absorption by intestinal epithelial cells, the fat-soluble nutrients, embedded in the carriers, need to be released from carriers firstly, and penetrated into mixed micelles or vesicles.[3] Seen from the digestive pathways in the body, it was found that the amount of fat-soluble nutrients transferred from food to the micellar phase was the key parameter, which determines absorption levels of nutrients by small intestine.[44] Therefore, the degree of micellization was a key parameter to characterize the bioaccessibility of fat-soluble nutrients *in vitro* digestion.

Many studies have proved that the OSA modified starch emulsions showed the great benefits on bioaccessibility of β-carotene. When the lipid layers were hydrolyzed gradually, more and more β-carotenes were released from the oil droplets. Meanwhile, many free fatty acids are produced during the hydrolysis of lipid, which could penetrate the mixed micelles. This could give rise to the higher solubility of β-carotenes in the mixed micelles.[17,18] Besides, the higher DS of OSA modified starch may be beneficial to the stability of the emulsion in the digestive tract, which resulted in the more β-carotenes were released from oil droplets.[30] Inspired by the better bioaccessibility caused by OSA modified starch, the bioaccessibility of β-carotene in the OSA@NS and OSA@PS emulsions with different DS were measured in detail, as shown in Fig. 9. It was found that availability of β-carotene enhanced along with the increasing DS of OSA modified starches, which was consistent with previous studies.[18,30,45] For example, 5% OSA@PS sample have the excellent bioaccessibility, due to the DS up to 0.0289. Compared with OSA@NS samples, the bioaccessibility of OSA@PS emulsions showed almost twice than that of OSA@NS. As far as we know, there is still no report on the OSA modified porous starch. Moreover, OSA modified starch exhibited well-stabilizing effect for β-carotene. Therefore, OSA modified PS, which can obtain the higher DS than the native one, indeed was an excellent alternative for stabilize β-carotene emulsions.

In summary, OSA modified porous starches with different DS were synthesized successfully by esterification reaction between porous starch and OSA groups. The spectra of ^{13}C solid-state NMR and FT-IR spectroscopy confirmed that ester linkage of

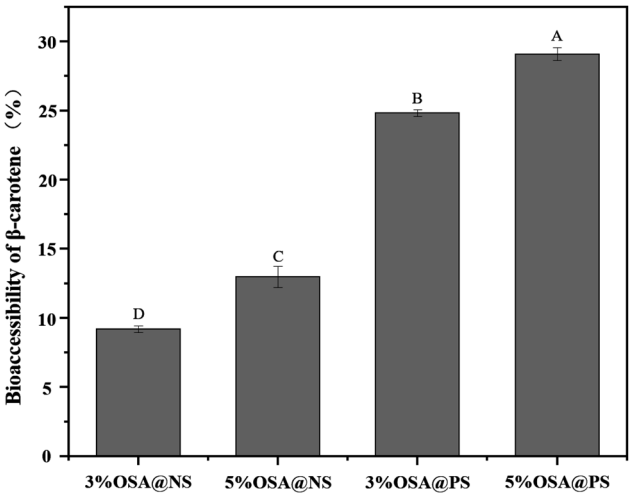

Fig. 9 Bioaccessibility of β-carotene embedded in the emulsions after digestion *in vitro*. Different capital letters indicate a statistically significant difference ($p < 0.01$).

OSA modified PS was successfully formed. The XRD patterns and SEM images suggested that the ordered crystalline configuration and porous structure of starch granules were not destroyed during the OSA modified process. Using the lower consumptions of PS as materials, the higher DS of OSA@PS with the DS of 0.0289 was obtained. Furthermore, OSA@PS possessing the excellent ability of emulsification was applied as an emulsion of β-carotene for the first time. In the simulated gastric juice, we found that the emulsions with the larger DS exhibited the less flocculation and coalescence, and the stability of the emulsion was positively correlated with the DS of OSA modified starch. It was also demonstrated that different DS of samples showed the great influences on the bioaccessibility of β-carotene in the emulsion, due to the variation of stability and particle sizes of the emulsions. Therefore, as a delivery system of food-grade, OSA@PS with higher DS could be applied as emulsions for stabilizing bioactive components.

Conflicts of interest

The authors declare no competing financial interest.

Acknowledgements

This work was financially supported by the National Natural Science Foundation of China (No. 21965002), the Scientific Research Start-up Funds of Gansu Agricultural University (No. 2017RCZX-46) and Modern Agricultural Industry Technology System of Gansu Province (No. GARS-TSZ-4). The authors thank Prof. Wei Wang (Lanzhou University) for the assistance with ^{13}C solid state NMR analysis and beneficial discussion.

References

1 A. V. Rao and L. G. Rao, *Pharmacol. Res.*, 2007, **55**, 207–216.

2 Y. Yonekura and A. Nagao, *Mol. Nutr. Food Res.*, 2007, **51**, 107–115.
3 R. Liang, C. F. Shoemaker, X. Yang, F. Zhong and Q. Huang, *J. Agric. Food Chem.*, 2013, **61**, 1249–1257.
4 C. S. Boon, D. J. McClements, J. Weiss and E. A. Decker, *Crit. Rev. Food Sci. Nutr.*, 2010, **50**, 515–532.
5 E. Meroni and V. Raikos, *Food Funct.*, 2018, **9**, 320–330.
6 Q. Lin, R. Liang, F. Zhong, A. Ye, Y. Hemar, Z. Yang and H. Singh, *J. Agric. Food Chem.*, 2019, **67**, 6614–6624.
7 C. P. Tan and M. Nakajima, *Food Chem.*, 2005, **92**, 661–671.
8 Y. Yuan, Y.-X. Gao, L. Mao and J. Zhao, *Food Chem.*, 2008, **107**, 1300–1306.
9 Y. Yuan, Y.-X. Gao, J. Zhao and L. Mao, *Food Res. Int.*, 2008, **41**, 61–68.
10 D. J. McClements and J. Rao, *Crit. Rev. Food Sci. Nutr.*, 2011, **51**, 285–330.
11 B. Ozturk and D. J. McClements, *Curr. Opin. Food Sci.*, 2016, **7**, 1–6.
12 J. Yi, Y. Li, F. Zhong and W. Yokoyama, *Food Hydrocolloids*, 2014, **35**, 19–27.
13 T. A. J. Verrijssen, L. G. Balduyck, S. Christiaens, A. M. Van Loey, S. Van Buggenhout and M. E. Hendrickx, *Food Res. Int.*, 2014, **57**, 71–78.
14 M. C. Sweedman, M. J. Tizzotti, C. Schafer and R. G. Gilbert, *Carbohydr. Polym.*, 2013, **92**, 905–920.
15 O. Torres, B. Murray and D. A. Sarkar, *Trends Food Sci. Technol.*, 2016, **55**, 98–108.
16 J. He, J. Liu and G. Zhang, *Biomacromolecules*, 2008, **9**, 175–184.
17 S. Zhao, G. Tian, C. Zhao, C. Lu, Y. Bao, X. Liu and J. Zheng, *Food Hydrocolloids*, 2018, **85**, 248–256.
18 Q. Lin, R. Liang and F. Zhong, *Food Hydrocolloids*, 2017, **73**, 184–193.
19 Q. Lin, R. Liang, F. Zhong, A. Ye and H. Singh, *Food Hydrocolloids*, 2018, **84**, 303–312.
20 H. Ruan, Q. Chen, M. Fu, Q. Xu and G. He, *Food Chem.*, 2009, **114**, 81–86.
21 F. Gao, D. Li, C. Bi, Z. Mao and B. Adhikari, *Carbohydr. Polym.*, 2014, **103**, 310–318.
22 X. Ma, X. Liu, D. P. Anderson and P. R. Chang, *Food Chem.*, 2015, **181**, 133–139.
23 P. R. Chang, D. Qian, D. P. Anderson and X. Ma, *Carbohydr. Polym.*, 2012, **88**, 604–608.
24 A. Dura, W. Blaszczak and C. M. Rosell, *Carbohydr. Polym.*, 2014, **101**, 837–845.
25 B. Zhang, D. Cui, M. Liu, H. Gong, Y. Huang and F. Han, *Int. J. Biol. Macromol.*, 2012, **50**, 250–256.
26 X. Song, G. He, H. Ruan and Q. Chen, *Starch*, 2006, **58**, 109–117.
27 M. J. Tizzotti, M. C. Sweedman, D. Tang, C. Schaefer and R. G. Gilbert, *J. Agric. Food Chem.*, 2011, **59**, 6913–6919.
28 S. J. Hur, E. A. Decker and D. J. McClements, *Food Chem.*, 2009, **114**, 253–262.
29 A. Sarkar, K. Goh, R. P. Singh and H. Singh, *Food Hydrocolloids*, 2009, **23**, 1563–1569.
30 L. Salvia-Trujillo, C. Qian, O. Martín-Belloso and D. J. McClements, *Food Chem.*, 2013, **141**, 1472–1480.
31 Y. Zheng, L. L. Hu, N. Ding, P. Liu, C. Yao and H. X. Zhang, *Int. J. Biol. Macromol.*, 2017, **94**, 566–570.
32 R. Bhosale and R. Singhal, *Carbohydr. Polym.*, 2007, **68**, 447–456.
33 F. Ye, M. Miao, C. Huang, K. Lu, B. Jiang and T. Zhang, *J. Agric. Food Chem.*, 2014, **62**, 11696–11705.
34 Y. J. Bai, Y. C. Shi, A. Herrera and O. Prakash, *Carbohydr. Polym.*, 2011, **83**, 407–413.
35 Z. Liu, Y. Li, F. Cui, L. Ping, J. Song, Y. Ravee, L. Jin, Y. Xue, J. Xu, G. Li, Y. Wang and Y. Zheng, *J. Agric. Food Chem.*, 2008, **56**, 11499–11506.
36 S. Tian, Z. Wang, X. Wang and R. Zhao, *RSC Adv.*, 2016, **6**, 96182–96189.
37 W. Liu, Y. Li, M. Chen, F. Xu and F. Zhong, *J. Agric. Food Chem.*, 2018, **66**, 9301–9308.
38 G. He, X. Song, H. Ruan and F. Chen, *J. Agric. Food Chem.*, 2006, **54**, 2775–2779.
39 M. Lopez-Silvaa, L. A. Bello-Pereza, E. Agama-Acevedoa and J. Alvarez-Ramirezb, *Food Hydrocolloids*, 2019, **97**, 105–212.
40 J. Wang, L. Su and S. Wang, *J. Sci. Food Agric.*, 2009, **90**, 424–429.
41 D. J. McClements and H. Xiao, *Food Funct.*, 2012, **3**, 202–220.
42 K. Królikowska, S. Pietrzyk, T. Fortuna, P. Pająk and M. Witczak, *Food Chem.*, 2019, **278**, 284–293.
43 H. Zhang, C. Schäfer, P. Wu, B. Deng, G. Yang, E. Li, R. G. Gilbert and C. Li, *Food Hydrocolloids*, 2018, **74**, 168–175.
44 P. Wang, H. J. Liu, X. Y. Mei, M. Nakajima and L. J. Yin, *Food Hydrocolloids*, 2012, **26**, 427–433.
45 S. Kokubun, I. Ratcliffe and P. A. Williams, *Carbohydr. Polym.*, 2018, **194**, 18–23.